state. The internal monomer concentration is then independent of molecular weight and depends solely on the balance between steric repulsions and van der Waals attractions. The transition can be described with reasonable accuracy by the thermal blob model.

It must be pointed out, however, that several difficulties remain to be solved: (1) The need to use slightly different $n\alpha M_0$ values for polystyrene in cyclopentane and cyclohexane is not in agreement with a universal behavior. It is not clear yet if this discrepancy arises from our limited experimental accuracy or is more fundamental. (2) The average $n\alpha M_0$ value of 150 ± 30 g mol^{-1} in the collapsed state is much lower than the measured corresponding value of 1000 ± 50 g mol^{-1} previously found in the extended state. This difference may reflect the influence of the higher than binary interactions in the collapsed state. (3) The slight residual molecular weight dependence in our universal plots is not accounted for by the theory. (4) So far, the molecular weight dependence of the hydrodynamic radius characteristic of the collapsing regime has been proved only at a single temperature. This should be repeated at several different temperatures.

When applicable, the comparison of the present data with the literature shows a good agreement in general. There are however two notable exceptions that both correspond to attempts to reach the totally collapsed regime in which the hydrodynamic radius of the globular chain saturates to its minimum value. The disagreement is very serious for the Prague group while it is probably only qualitative for the MIT group. These experiments should be repeated especially in view of the fact that the light scattering technique allows use of lower concentrations than the present sedimentation experiments. The accessible temperature range is then sufficiently large to cover the entire coil–globule transition. Last, to test the eventual superiority of the mean-field theory over the blob model, it would be very interesting to work on polymers of various flexibility since only the former approach includes this important parameter.

Registry No. Polystyrene, 9003-53-6.

References and Notes

(1) P. Vidakovic and F. Rondelez, *Macromolecules*, **16**, 253 (1983).
(2) P. Vidakovic and F. Rondelez, *Macromolecules*, submitted for publication.
(3) C. Williams, F. Brochard, and H. Frisch, *Ann. Rev. Phys. Chem.*, **32**, 433 (1981).
(4) M. Nierlich, J. P. Cotton, and B. Farnoux, *J. Chem. Phys.*, **69**, 1379 (1978).
(5) R. Perzynski, M. Adam, and M. Delsanti, *J. Phys. (Orsay, Fr.)*, **43**, 129 (1982).
(6) E. L. Slagowski, B. Tsai, and D. McIntyre, *Macromolecules*, **9**, 687 (1976).
(7) M. J. Pritchard and R. D. Caroline, *Macromolecules*, *13*, 957 (1980).
(8) D. R. Bauer and R. Ullman, *Macromolecules*, **13**, 392 (1980).
(9) G. Swislow, S. T. Sun, I. Nishio, and T. Tanaka, *Phys. Rev. Lett.*, **44**, 796 (1980).
(10) S. T. Sun, I. Nishio, G. Swislow, and T. Tanaka, *J. Chem. Phys.*, **73**, 5971 (1980).
(11) P. Štěpánek, C. Koňák, and B. Sedláček, *Macromolecules*, **15**, 1214 (1982).
(12) O. B. Ptitsyn, A. K. Kron, and Y. Y. Eizner, *J. Polym. Sci., Part C*, **16**, 3509 (1968).
(13) P. G. de Gennes, *J. Phys., Lett. (Orsay, Fr.)*, **36**, L-55 (1975).
(14) I. C. Sanchez, *Macromolecules*, **12**, 980 (1979).
(15) M. Daoud and J. Jannink, *J. Phys. (Orsay, Fr.)*, **37**, 973 (1976).
(16) P. G. de Gennes, *J. Phys., Lett. (Orsay, Fr.)* **39**, L-299 (1978).
(17) G. Weill and J. des Cloizeaux, *J. Phys. (Orsay, Fr.)*, **40**, 99 (1979).
(18) A. Z. Ackasu and C. C. Han, *Macromolecules*, **12**, 276 (1979).
(19) See for example: C. Post and B. Zimm, *Biopolymers*, **18**, 1487 (1979), and also ref (13).
(20) M. A. Moore, *J. Phys. A*, **10**, 305 (1977).
(21) P. Vidakovic, C. Allain, and F. Rondelez, *Macromolecules*, **15**, 1571 (1982).
(22) B. Nyström, J. Roots, and R. Bergman, *Polymers*, **20**, 157 (1979).
(23) M. Adam and M. Delsanti, *J. Phys. (Orsay, Fr.)*, **41**, 713 (1980).
(24) G. Pouyet, F. Candau, and J. Dayantis, *Makromol. Chem.*, **177**, 2973 (1976).
(25) D. Sarazin and J. François, *Polymers*, **19**, 699 (1978).
(26) M. Schmidt and W. Burchard, *Macromolecules*, **14**, 210 (1981).
(27) M. Adam, private communication. See also: N. Kuwahara, M. Tachikawa, K. Hamano, and Y. Kenmochi, *Phys. Rev.*, **A25**, 3449 (1982).

Dynamic Light Scattering Studies of Polymer Solutions. 3. Translational Diffusion and Internal Motion of High Molecular Weight Polystyrenes in Benzene at Infinite Dilution

Norio Nemoto, Yutaka Makita, Yoshisuke Tsunashima, and Michio Kurata*

Institute for Chemical Research, Kyoto University, Uji, Kyoto-fu 611, Japan.

Received February 24, 1983

ABSTRACT: Dynamic light scattering studies have been made on dilute solutions of narrow-distribution polystyrenes in benzene at 30 °C over a wide range of qR_G ($\equiv X^{1/2}$). The intensity autocorrelation function has been analyzed with the histogram method. The analysis made it possible to estimate the translational diffusion coefficient D, the effective decay rate Γ_e, and the intensity of the translational diffusion motion relative to the total intensity P_0/P at finite polymer concentration. Those quantities have been linearly extrapolated to infinite dilution to obtain values characteristic of a single swollen coil. It has been found that the hydrodynamic radius R_H calculated from D_0 increases in proportion to $M_w^{0.55}$ and expansion factors α_H and α_s have different functional dependences on the excluded volume parameter z. It has also been found that, for $X^{1/2} \gg 1$, the quantity $(\Gamma_e)_{c\to 0}/(q^3 k_B T/\eta_0)$ approaches a constant value which is less than the theoretical value by 25%. The X dependence of $(P_0/P)_{c\to 0}$ suggests that the internal motion is suppressed in a single swollen coil to some extent in comparison with that in a Gaussian coil. The concentration dependence of D is also briefly discussed.

Introduction

In a previous report,[1] we have investigated dynamics of dilute solutions of narrow-distribution polystyrenes (PS) in *trans*-decalin at the Θ temperature over a wide range of $qR_G \equiv X^{1/2}$ by means of homodyne photon correlation spectroscopy. Here q is the scattering vector and R_G is the radius of gyration. We have found that the dynamical behavior of an isolated unperturbed chain is quantitatively

0024-9297/84/2217-0425$01.50/0

described by Zimm's nondraining bead–spring model except a 15% difference between hydrodynamic radii calculated from values of translational diffusion coefficients D_0 and theoretical values. It has been suggested that this disagreement is due to the improper theoretical treatment of hydrodynamic interaction between constituting monomeric units or polymer segments.

For dynamics of flexible polymers in good solvents, the effect of the excluded volume must be taken into account in addition to the effect of the hydrodynamic interaction. There have been attempts to elucidate the excluded volume effect on the molecular weight dependence of D_0 obtained in the small q region characterized by $X^{1/2} \ll 1$.[2,3] Since the intermediate scattering function $A(q,t)$ deviates from a single-exponential type of decay in the range of $X^{1/2} \geq 1$ due to contribution of intramolecular motions, reliable data were limited to D_0 of low molecular weight samples. Adam and Delsanti[4] have extended dynamic light scattering (DLS) experiments up to the intermediate q region defined by $X^{1/2} > 1$ but $ql < 1$, where l is the statistical length. Their work has been mainly concerned with the scaling property of $A(q,t)$ in the asymptotic q region where the theory of Dubois-Voillette and de Gennes[29] may be applied. Only the power dependence of the characteristic frequency $\omega_c(q)$ in $A(q,t) \equiv \exp[f(\omega_c t)]$ has been discussed.

Recently, Akcasu et al.[5] have developed an excellent method for the interpretation of DLS experiments made under a variety of experimental conditions, in terms of the first cumulant $\Omega(q)$ of $A(q,t)$. This method is quite useful for the test of various molecular models which accounted for the hydrodynamic interaction as well as the excluded volume effect. Han and Akcasu[6] have compared theoretical predictions with results of DLS measurements on dilute solutions of high molecular weight PS samples in toluene in the intermediate q region. They have shown that the dependence of Ω on q is in agreement with their theory as far as the general trend is concerned but somewhat less satisfactory with respect to quantitative agreement. Unfortunately, their data have not been extrapolated to infinite dilution where comparison between theories and experiments should be made. Further, values of $D \equiv (\Omega(q)/q^2)_{q\to 0}$ have not been estimated for high molecular weight samples because of experimental difficulties. Thus their conclusions seem to leave room for further discussion.

In this paper, we present DLS studies on dilute solutions of high molecular weight PS samples in benzene. Autocorrelation function data were analyzed with the histogram method. The analysis made it possible to estimate D_0, effective decay rate Γ_e which is equivalent to Ω, and also the relative intensity of the translational diffusion motion to the total scattered intensity at infinite dilution with high accuracy. Those quantities have been used to test several molecular theories on dynamics of a single polymer chain in good solvent.

Experimental Section

Materials. Five samples of narrow-distribution polystyrenes (PS) with M_w ranging from 7.75×10^5 to 1.34×10^7 were used for the present study. Four samples with higher M_w have been characterized with methods of static light scattering and GPC by Fukuda et al.[7] M_w and M_w/M_n of the lowest molecular weight sample F80 have been obtained in this laboratory.[8] Their characteristics are shown in Table I. Spectrograde benzene (Nakarai Chemicals) has been used as solvent without further purification.

Method. The dynamic light scattering instrument used has been described in detail elsewhere.[9] Dilute solutions of PS in benzene were prepared for DLS measurements as follows. Most concentrated solutions were first prepared by dissolving the polymer into dust-free benzene and made optically clean by either ultracentrifugation for two high molecular weight samples (FF36, FF37) or filtration with Millipore filters (nominal pore size, 0.22 μm) for the other three samples. The solutions were diluted with dust-free benzene to obtain at least four solutions with different concentrations for respective samples. Concentrations were determined by weighing.

The intensity autocorrelation function $A(\tau)$ of solutions was measured at 30.0 ± 0.02 °C by either a time interval method (512 channels) or a shift register method (Malvern, 72 channels) of homodyne photon correlation spectroscopy. A single-frequency 488-nm line of an argon ion laser (Spectra Physics Model 165-03) was used as the light source. The vertical component of the light scattered from solutions in sample cells (NMR tube, o.d. 12 mm) was detected by photomultipliers (Hamamatsu TV) at six fixed scattering angles of 10°, 30°, 60°, 90°, 120°, and 150°. The histogram analysis of data was made by using a Facom M160 AD computer at this institute.

Table I
Characterization of PS (Benzene, 30 °C)

sample	$10^{-6}M_w$	10^4A_2, mol cm^3 g^{-2}	$10^{11}R_G^2$, cm^2	M_w/M_n
F80	0.775	3.25[a]		1.01
FF33	2.42	2.33	6.25	1.04
FF35	5.53	1.89	15.8	1.04
FF36	9.70	1.60	30.1	1.03
FF37	13.4	1.50	44.5	

[a] Calculated from an empirical relation, $A_2 = 1.45 \times 10^{-2}M_w^{-0.28}$ (ref 7).

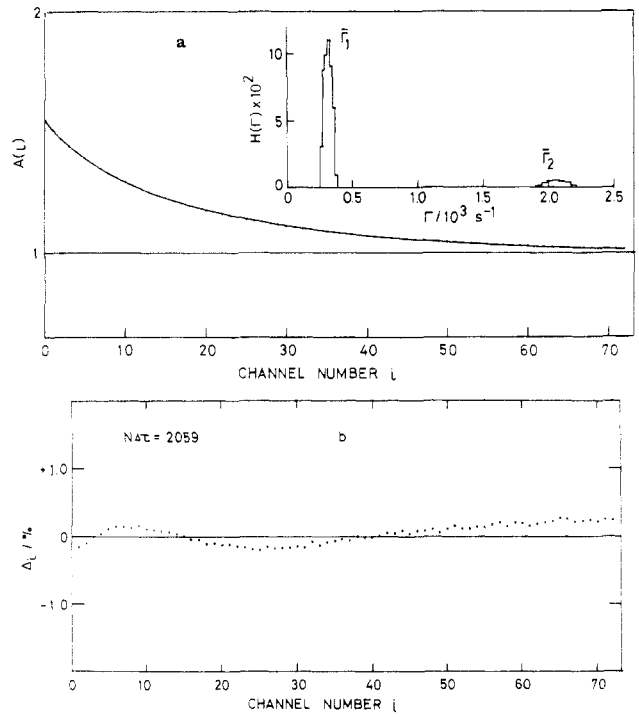

Figure 1. (a) Example of normalized $A(\tau)$ data obtained for the solution of the highest molecular weight sample (FF37) in benzene with $c = 1.53 \times 10^{-4}$ g cm^{-3} at $\theta = 30°$, ST = 70 μs, and the sampling number $N = 2.94 \times 10^7$. The insert in the figure shows the result of the histogram analysis on this $A(\tau)$ data. The solid curve is the fitting curve calculated by using the $H(\Gamma)$ in the insert. (b) Corresponding error of fit plot.

Results and Discussion

Data Analysis and Extrapolation to Infinite Dilution. All data except those of solutions of the lowest molecular weight samples (F80) were analyzed with the histogram method, whose validity was amply demonstrated in previous papers.[1,9,10] Figure 1 gives an example of $A(\tau)$ data which was obtained for the solution of the highest

molecular weight sample (FF37) in benzene with $c = 1.53 \times 10^{-4}$ g cm^{-3} at scattering angle $\theta = 30°$ and sampling time ST = 70 μs. The insert in the figure shows the result of the histogram analysis of this $A(\tau)$ data. The distribution of decay rate Γ, $G(\Gamma)$, is expressed by two peaks well separated from each other, as is anticipated from the value of $X = 4.48$ calculated from R_G of this sample and the scattering angle.[30] A component with lower decay rate $\bar{\Gamma}_1$ may be assigned as the translational diffusion mode and the second one with higher decay rate $\bar{\Gamma}_2$ as the internal mode. Thus the histogram method makes it possible to estimate the translational diffusion coefficient D with high precision from data obtained for X larger than unity by averaging Γ with $G(\Gamma)$ over the slow component only. An effective decay rate Γ_e defined by eq 1 and the intensity of the slow component P_0 relative to the sum of the slow and fast component P may be also estimated by the histogram analysis.

$$\Gamma_e = \int_0^\infty \Gamma G(\Gamma)\, d\Gamma = \sum_{j=1}^{L} \Gamma_j H_j(\Gamma_j) \Delta\Gamma \quad (1)$$

$$\sum_{j=1}^{L} H_j(\Gamma_j)\Delta\Gamma = 1 \quad (2)$$

Here $H_j(\Gamma_j)$ is the histogram step height, whose Γ_j is between $\Gamma_j + \Delta\Gamma/2$ and $\Gamma_j - \Delta\Gamma/2$, and L the number of histogram steps. P_0/P is obtained as the sum of $H_j(\Gamma_j)\Delta\Gamma$, whose Γ_j is included in the Γ region of the slow component. For $X^{1/2} \ll 1$, $G(\Gamma)$ takes a unimodal distribution and Γ_e may be put equal to Dq^2. For $X^{1/2} \gg 1$, Γ_e mainly reflects the internal motion. For X less than about 10, P_0/P represents the relative intensity of the translational mode to the total intensity but may lose such a physical meaning for much larger X, where mixing of the translational and the internal modes takes place.[31]

D values of the solutions of F80 were estimated by fitting $A(\tau)$ data to curves of a single-exponential decay type. For all solutions of the remaining four polymer samples, the histogram analysis on $A(\tau)$ data obtained at $\theta = 10°$ gave unimodal Γ distributions. This tempted us, at first, to calculate D by using Γ_e values obtained at 10°. However, $X^{1/2}$ is 0.713 at $\theta = 10°$ for the highest molecular weight sample FF37, and the theory by Akcasu et al.[5] predicts that D calculated from Γ_e with $X^{1/2} \simeq 0.7$ is larger than the true D value at $X^{1/2} \to 0$ by several percent. We calculated D of solutions of FF37 from the slow component of the Γ distribution obtained for the data at $\theta = 30°$ ($X^{1/2} = 2.12$), for comparison with D at 10°. The former values were found to be less than the latter values by about 2%, independent of polymer concentration. The 2% difference is well within an error of 5% which occurs in the application of the histogram method on a decay curve with a bimodal distribution of Γ. This difference is also less than an error of 2.5% expected from the consideration of the optical alignment at $\theta = 10°$. Therefore we took an average of D obtained at $\theta = 10°$ and 30° as the D value of the solution of FF37 at each concentration. A similar averaging was made for solutions of FF36, and D at 10° was assumed very close to the true value for solutions of FF33 and FF35.

Figure 2 shows the concentration dependence of D thus obtained. The data are well represented by straight lines, from which D_0 and k_D in eq 3 can be estimated. Values

$$D = D_0(1 + k_D c) \quad (3)$$

of D_0 and k_D are listed in Table II, and the dependence of D_0 on M_w was expressed by eq 4.

$$D_0 = 2.46 \times 10^{-4} M_w^{-0.55\pm0.22} \quad (4)$$

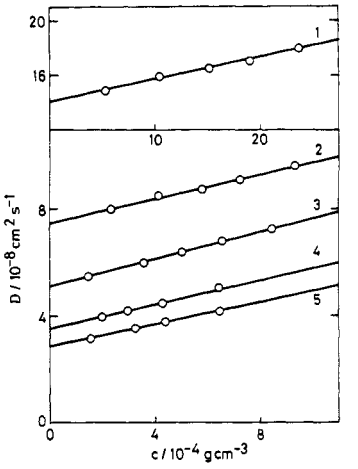

Figure 2. Concentration dependence of the translational diffusion coefficients D. The digit 1 denotes F80; 2, FF33; 3, FF35; 4, FF36; 5, FF37.

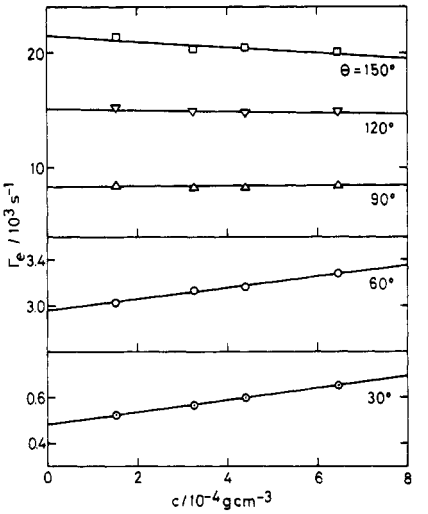

Figure 3. Linear extrapolation of Γ_e obtained for the solutions of FF37 to infinite dilution at five scattering angles from 30° to 150°.

Table II
Experimental Results of D_0, k_D, and R_H

sample	$10^8 D_0$, cm^2 s^{-1}	k_D, cm^3 g^{-1}	$10^6 R_H$,[a] cm
F80	14.1	120	2.80
FF33	7.45	310	5.29
FF35	5.12	490	7.70
FF36	3.53	640	11.2
FF37	2.84	740	13.9

[a] R_H was calculated from D_0 by using eq 5.

Figure 3 gives an example of the concentration dependence of Γ_e at constant q values obtained for solutions of FF37. The data are well represented by straight lines, and thus extrapolation to infinite dilution can be made quite easily. It is interesting that, with increasing $X^{1/2}$, slopes change sign from a positive to a slightly negative value. This is in contrast to negative concentration dependences of Γ_e at the Θ temperature for all $X^{1/2}$ values.[1] Positive slopes at 30° and 60° may be attributed to the positive c dependence of the translational diffusion motion. The negative one at 150° may be related to the decrease in relaxation times of the internal molecular motions with decreasing c.

Figure 4 gives the concentration dependence of P_0/P obtained for solutions of FF33. The data at 30° gave a

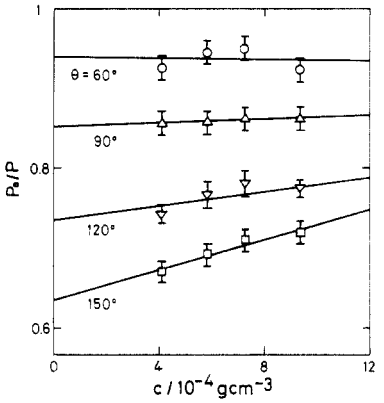

Figure 4. Linear extrapolation of P_0/P obtained for the solutions of FF33 to infinite dilution at four angles from 60° to 150°.

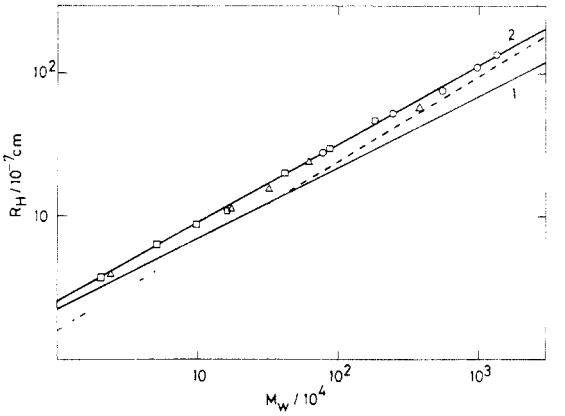

Figure 5. Logarithmic plot of R_H against M_w: (solid line 1) R_H of PS in *trans*-decalin, eq 8; (solid line 2) R_H of PS in good solvents, eq 9; (dotted line) R_H calculated by using eq 6; (○) this work; (△) data obtained by Adam and Delsanti;[4] (□) data by Mandema and Zeldenrust.[11]

unimodal Γ distribution, which resulted in $P_0/P = 1$. P_0/P values at respective q are linearly dependent on c within experimental error. Therefore $(P_0/P)_{c\to 0}$ could be determined within several percent. There is no theoretical guide to explain the increase in slope of solid lines with increasing X. It may be noted that the present study is the first to extrapolate Γ_e and P_0/P to $c = 0$ for polymer solutions where $M > 4 \times 10^6$.

Translational Diffusion Motion. There have been a couple of studies[4,11] that have investigated the molecular weight dependence of D_0 for PS–good solvent systems or that of the equivalent hydrodynamic radius R_H defined by eq 5.

$$R_H = k_B T/6\pi\eta_0 D_0 \tag{5}$$

Here η_0 is the solvent viscosity and $k_B T$ has its usual meaning. In the range of M from 20 400 to 3 800 000 investigated by those studies, D_0 was found to decrease with $M^{-0.55\pm0.22}$, which agrees with the present data. This molecular weight dependence is weaker compared with that of R_G, well established both theoretically and experimentally in the good solvent limit. In order to check quantitative agreement between earlier and our present data, we plot R_H rather than D_0 against M_w in Figure 5, since R_H is not affected much by the difference in either temperature or solvent viscosity used for respective investigations. In the figure, we include a theoretical prediction with the dotted line, which is calculated by using eq 6.

$$R_H = R_G/6\pi Q = 6.60 \times 10^{-10} M_w^{0.595\pm0.005} \tag{6}$$

This equation is obtained by combining a theoretical relation between R_H and R_G in the good solvent limit[5] and an empirical relation between R_G and M_w[12]

$$R_G^2 = (1.47 \pm 0.05) \times 10^{-18} M_w^{1.19\pm0.01} \tag{7}$$

We also show the previous result[1] obtained for PS in *trans*-decalin at the Θ temperature by the solid line 1.

$$R_{H,\Theta} = 2.21 \times 10^{-9} M_w^{0.50} \tag{8}$$

Evidently, all data points are located above the solid line 1 as is expected. Also our data look to connect smoothly with low molecular weight data and to form a single straight line which may be expressed as

$$R_H = 1.60 \times 10^{-9} M_w^{0.55} \tag{9}$$

On the other hand, this line does not coincide with the theoretical line, and discrepancies are much larger than experimental uncertainties. A theory has been proposed by Weill and des Cloizeaux[13] to reconcile the discrepancy in values of the exponent between R_G–M_w and R_H–M_w relationships. They have argued that R_G approaches the limiting behavior of $M \to \infty$ much faster than R_H does, and thus the above discrepancy has arised from the finiteness of molecular weights of samples investigated. The highest molecular weight of samples examined in the present study is 1.34×10^7, and this may not be sufficient to observe the asymptotic behavior for R_H as they claim. Nevertheless it was difficult to conceive any trend toward such a limiting behavior from the data.

The two-parameter theory[14] of flexible polymers in dilute solutions indicates that expansion factors α_s and α_H defined by eq 10 and 11 may have different molecular

$$\alpha_s = R_G/R_{G,\Theta} \tag{10}$$

$$\alpha_H = R_H/R_{H,\Theta} \tag{11}$$

weight dependences. First-order perturbation theories predict[15-17] that α_H is smaller than α_s for positive values of the excluded volume parameter z defined by eq 12.

$$z = (1/4\pi)^{3/2}(\beta/M_0^2)(M/R_{G,\Theta})^{3/2} M^{1/2} \tag{12}$$

Here M_0 is the molecular weight of a repeat unit of the polymer and β is the binary cluster integral for interaction between repeat units. On the other hand, relationships between expansion factors and z in the good solvent limit are not derived yet. Static light scattering experiments by Miyaki et al.[12] have shown that eq 13 closely approx-

$$\alpha_s^2 = 1.53 z^{2/5} \tag{13}$$

imates the behavior of α_s of high molecular weight PS in benzene with reference to $R_{G,\Theta}$ in cyclohexane.

If the effect of the hydrodynamic interaction is independent of solvent power as proved in a later section, α_H may be also a universal function of z, and its functional dependence can be derived from the data in Figure 5 along with the value of z estimated from static light scattering data. To be consistent with the diffusion data, α_s in eq 10 was recalculated by using $R_{G,\Theta}$ in *trans*-decalin at the Θ temperature. z was then given as $z = 3.53 \times 10^{-3} M_w^{0.5}$ from the α_s–M_w relation and eq 13. α_H was obtained from R_H data shown in Figure 5 and $R_{H,\Theta}$ estimated by eq 8. From the plot of α_H against z, we obtained

$$\alpha_H = 1.27 z^{0.1} \tag{14}$$

From the comparison of eq 14 and 13, we see that α_H is much smaller than α_s in the region of large molecular weight where z becomes large. Equation 14 may be tested in the future development of the two-parameter theory.

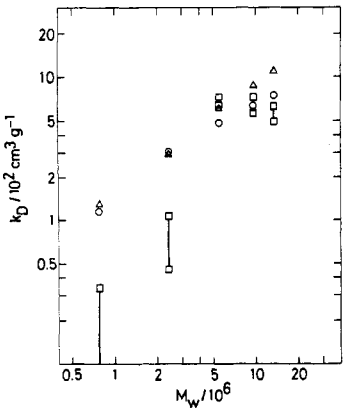

Figure 6. Logarithmic plot of k_D against M_w: (○) experimental data; (△) theoretical values by Yamakawa theory, eq 15; (□) theoretical values by PF–M theory, eq 16.

Figure 6 gives the double-logarithmic plot of k_D values (○) listed in the fourth column of Table II against M_w. Theoretical values of k_D (△, □) calculated by using eq 15 and 16, respectively, are shown in the figure for compar-

$$k_D = 0.8A_2M - N_A v_H/M - \bar{v} \quad \text{(Yamakawa theory)}^{18} \tag{15}$$

$$k_D = 2A_2M - B(N_A v_H/M) - \bar{v} \quad \text{(PF–M theory)}^{19,20} \tag{16}$$

ison. In the calculation, A_2 and M values were taken from Table I, hydrodynamic volume v_H was calculated by assuming $v_H = (4\pi/3)R_H^3$, the partial specific volume of the polymer $\bar{v}$ was put equal to 1.1 cm^3 g^{-1}, and N_A is the Avogadro number. B in the PF–M theory ranges from 6.55[20] to 7.01[19], leading to some allowance for k_D as indicated by error bars. In a relatively low molecular weight range, the Yamakawa theory seems to give better agreement with experiments than the PF–M theory. Recent results of DLS measurements[21] on dilute solutions of PS with $M < 2 \times 10^6$ in good solvent also support the Yamakawa theory. For $M > 5 \times 10^6$, on the other hand, k_D values agree semiquantitatively with either theoretical value. It has been shown for PS in *trans*-decalin that, at the Θ state, the molecular weight dependence of k_D, $k_D \propto M_w^{0.43}$, differs from the prediction of either the Y–I[22] or the PF–M theory, $k_D \propto M^{0.5}$, and absolute values obtained experimentally are larger than those of the Y–I theory but less than the PF–M theory. Small discrepancies in the good solvent between experiments and theories exhibit similar tendency as in the Θ solvent. This implies that the calculation of the hydrodynamic volume calculated by putting $v_H = (4\pi/3)R_H^3$ may be incorrect.

Effective Decay Rate $(\Gamma_e)_{c\to 0}$. Figure 7 shows the reduced plot of $(\Gamma_e)_{c\to 0}/(q^3k_BT/\eta_0)$ against $X^{1/2}$. The solid curve in the figure is the theoretical curve calculated for the nondraining flexible coil with a preaveraged Oseen tensor.[5] With increasing $X^{1/2}$, the reduced effective decay rate decreases monotonically and approaches a constant value for $X^{1/2} > 4$ asymptotically. The q^3 proportionality of Γ_e indicates that an isolated polymer chain can be represented by the nondraining model. Agreement between the theory and experiment is however only qualitative. The asymptotic Γ_e value is smaller than the theoretical value by about 25%. It should be noted that if a nonpreaveraged Oseen tensor is used in the calculation, the agreement becomes worse.

Recently, Han and Akcasu[6] estimated the first cumulant, or Γ_e in our notation, of PS in toluene with the method of the cumulant and found that their data came much closer to the theoretical prediction than ours. The difference between their data and our data may be ascribed to the following: (1) the former data were not extrapolated to infinite dilution but the data at finite concentrations were used for comparison with the theory and (2) the precision of cumulant analysis becomes poor when $X^{1/2}$ exceeds 2 as they noticed.

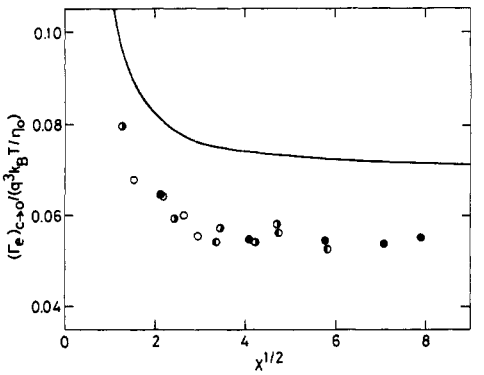

Figure 7. Plot of reduced effective decay rates $(\Gamma_e)_{c\to 0}/(q^3k_BT/\eta_0)$ against $X^{1/2}$: (○) FF33; (◑) FF35; (◐) FF36; (●) FF37. The solid curve is a theoretical curve calculated for the nondraining flexible coil with a preaveraged Oseen tensor in good solvent limit.

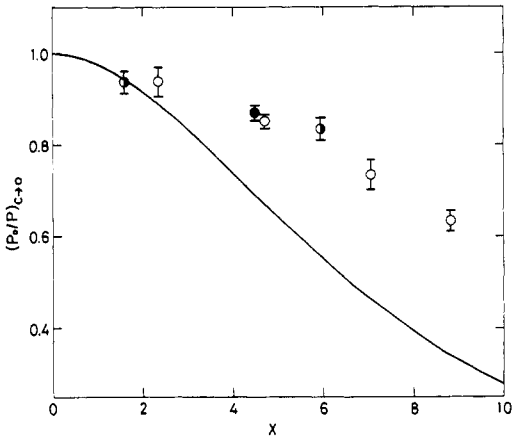

Figure 8. Dependence of the relative intensity $(P_0/P)_{c\to 0}$ against X. The symbols are the same as in Figure 7. The solid curve is a theoretical curve for an unperturbed flexible coil with dominant hydrodynamic interaction.[23]

The 25% difference between the theory and the experiment in the good solvent is larger than the 15% difference observed for the same polymer at the Θ state. In the latter system, D_0 was also found to be 15% smaller than the theoretical value. Therefore, when $(\Gamma_e)_{c\to 0}/D_0q^2$ was plotted against $X^{1/2}$, cancellation of the disagreements in both $(\Gamma_e)_{c\to 0}$ and D_0 brought forth quantitative agreement between the theory and the experiment. In the case of the good solvent, a similar plot did not improve the agreement much, but the data fell on the theoretical curve calculated for a single unperturbed flexible chain.

The present data indicate that not only the recalculation of D_0 but also the reconsideration of the internal motion responsible for the behavior in the intermediate q region are necessary. The smaller $(\Gamma_e)_{c\to 0}$ values may indicate that the theory overestimates magnitudes either of decay rates of the internal modes or of associated amplitudes. The analysis of the relative intensity data to be described in the next section favors the latter conjecture.

Relative Intensity $(P_0/P)_{c\to 0}$. Figure 8 shows the X dependence of the relative intensity at infinite dilution $(P_0/P)_{c\to 0}$ in the range of X where $(P_0/P)_{c\to 0}$ gives the amplitude of the translational diffusion motion relative to that of all molecular motions that give rise to concentration fluctuation. The solid curve is a theoretical curve

for an unperturbed flexible chain with dominant hydrodynamic interaction.[23] A theory taking into account the excluded volume effect is not proposed yet. It may be shown that an assumption of the uniform expansion gives the prediction identical with the solid curve.[24]

$(P_0/P)_{c\to 0}$ decreases with increasing X, as it must. However an upward departure from the solid curve occurs near the relatively small value of $X \simeq 2$ and deviations become bigger with increasing X. This behavior is in contrast to that of PS in *trans*-decalin, for which the data points have been located on the solid line up to $X \leq 5$. It has been shown by Utiyama et al.[25] and also Fukuda et al.[7] that dependence of the scattering function $P(X)$ of PS in benzene is closely represented up to $X < 10$ by the Debye function derived for a Gaussian chain. Therefore the upward departure of $(P_0/P)_{c\to 0}$ in the good solvent suggests that normal mode type motions responsible for intramolecular relaxation are more or less depressed in a swollen coil. This may be one of the reasons why $(\Gamma_e)_{c\to 0}$ takes values smaller than the theoretical predictions which assumed complete flexibility to the swollen coil.

The longest relaxation time τ_1 may be roughly estimated from data with $1 \leq X \leq 3$, since in this range of X, the term associated with τ_1 accounts for the greater part of the intramolecular contribution.[23] We obtained $\tau_1 = 210$ and 830 μs for FF33 and FF35, respectively. These values are compared with theoretical values calculated from eq 17,

$$\tau_1 = M\eta_0[\eta]/A_1RT \tag{17}$$

where $A_1 = 0.822$ for the free-draining bead–spring model[26] and 1.18 for the nondraining model.[27] By using an empirical relation between $[\eta]$ and M_w[28]

$$[\eta] = 7.8 \times 10^{-5} M_w^{0.75} \tag{18}$$

We obtain τ_1 for FF33 from eq 17 as

$$\tau_1 = 320\ \mu\text{s} \quad \text{(free-draining)}$$

$$\tau_1 = 220\ \mu\text{s} \quad \text{(nondraining)}$$

and for FF35 as

$$\tau_1 = 1340\ \mu\text{s} \quad \text{(free-draining)}$$

$$\tau_1 = 930\ \mu\text{s} \quad \text{(nondraining)}$$

Comparison of experimental values with theoretical values reconfirms that the nondraining model is adequate for describing dynamics of an isolated polymer molecule in good solvents.

Registry No. Polystyrene (homopolymer), 9003-53-6.

References and Notes

(1) Tsunashima, Y.; Nemoto, N.; Kurata, M. *Macromolecules* **1983**, *16*, 1184.
(2) Ford, N. C., Jr.; Karasz, F. E.; Owen, J. E. M. *Discuss. Faraday Soc.* **1970**, *49*, 228.
(3) King, T. A.; Knox, A.; McAdum, J. D. G. *J. Polym. Sci., Polym. Symp. Ed.* **1974**, *44*, 195.
(4) Adam, M.; Delsanti, M. *Macromolecules* **1977**, *10*, 1229.
(5) (a) Akcasu, A. Z.; Benmouna, M.; Han, C. C. *Polymer* **1980**, *21*, 866. (b) Benmouna, M.; Akcasu, A. Z. *Macromolecules* **1980**, *13*, 409.
(6) Han, C. C.; Akcasu, A. Z. *Macromolecules* **1981**, *14*, 1080.
(7) Fukuda, M.; Fukutomi, M.; Kato, Y.; Hashimoto, T. *J. Polym. Sci., Polym. Phys. Ed.* **1974**, *12*, 871.
(8) Kobayashi, T. Master's Thesis, Kyoto University, 1980.
(9) Nemoto, N.; Tsunashima, Y.; Kurata, M. *Polym. J. (Tokyo)* **1981**, *13*, 827.
(10) (a) Tsunashima, Y.; Nemoto, N.; Makita, Y.; Kurata, M. *Bull. Inst. Chem. Res., Kyoto Univ.* **1980**, *59*, 293. (b) Tsunashima, Y.; Nemoto, N.; Kurata, M. *Macromolecules* **1983**, *16*, 584.
(11) Mandema, W.; Zeldenrust, H. *Polymer* **1977**, *18*, 835.
(12) Miyaki, Y.; Einaga, Y.; Fujita, H. *Macromolecules* **1978**, *11*, 1180.
(13) Weill, G.; des Cloizeaux, J. *J. Phys. (Orsay, Fr.)* **1979**, *40*, 99.
(14) Yamakawa, H. "Modern Theory of Polymer Solutions"; Harper and Row: New York, 1971; Chapter 6.
(15) Stockmayer, W. H.; Albrecht, A. C. *J. Polym. Sci.* **1958**, *32*, 215.
(16) Horta, A.; Fixman, M. *J. Am. Chem. Soc.* **1968**, *90*, 3048.
(17) Kurata, M.; Yamakawa, H. *J. Chem. Phys.* **1958**, *29*, 311.
(18) Yamakawa, H. *J. Chem. Phys.* **1962**, *36*, 2995.
(19) Pyun, C. W.; Fixman, M. *J. Chem. Phys.* **1964**, *41*, 937.
(20) Mulderije, J. J. H. *Macromolecules* **1980**, *13*, 1207, 1526.
(21) Han, C. C.; Akcasu, A. Z. *Polymer* **1981**, *22*, 1165.
(22) Imai, S. *J. Chem. Phys.* **1970**, *52*, 4212.
(23) Perico, A.; Piaggio, P.; Cuniberti, C. *J. Chem. Phys.* **1975**, *62*, 2690.
(24) Unpublished calculation.
(25) Utiyama, H.; Tsunashima, Y.; Kurata, M. *J. Chem. Phys.* **1971**, *55*, 3133.
(26) Rouse, P. E. *J. Chem. Phys.* **1953**, *21*, 1272.
(27) Zimm, B. H. *J. Chem. Phys.* **1956**, *24*, 269.
(28) Einaga, Y.; Miyaki, Y.; Fujita, H. *J. Polym. Sci., Polym. Phys. Ed.* **1979**, *17*, 2103.
(29) Dubois-Voillette, E.; de Gennes, P.-G. *Physics (Long Island City, N.Y.)* **1967**, *3*, 181.
(30) There seems to remain some doubt about the reliability of the histogram method from the mathematical point of view of the ill-conditioned nature of the Laplace inversion problem as is encountered in the present analysis. We have tested the histogram method by using simulated autocorrelation function data $A(\tau)$ which has a bimodal distribution of decay rates very close to that shown in the insert of Figure 1 and contains random errors of 1.5% at each of 72 points. Following the standard procedure briefly described in the Appendix of ref 10b, we have been able to derive a bimodal distribution of decay rates $H(\Gamma)$ close to the original $H(\Gamma)$. Values of $\bar{\Gamma}_1$, $\bar{\Gamma}_2$, Γ_e, and also the relative intensity P_0/P have agreed with corresponding theoretical values within an error of 5%. This may indicate that the histogram method is practically quite useful, if the method is carefully applied for very precise data.
(31) For data with large X, say $X > 20$, the histogram analysis did not give a bimodal distribution, but a broad unimodal distribution with a bump in the smaller Γ side. In those cases, we did not make an attempt to estimate $\bar{\Gamma}_1$, $\bar{\Gamma}_2$, and P_0/P by separating the distributions into the two modes, but only made an estimate of Γ_e.